Large Eddy Simulation of an SD7003 Airfoil: Effects of Reynolds number and Subgrid-scale modeling

Paper

Sarlak Chivaee, Hamid

Published in:
Wake Conference 2017

Link to article, DOI:
10.1088/1742-6596/854/1/012040

Publication date:
2017

Document Version
Publisher's PDF, also known as Version of record

Large Eddy Simulation of an SD7003 Airfoil: Effects of Reynolds number and Subgrid-scale modeling

2017 J. Phys.: Conf. Ser. 854 012040

(http://iopscience.iop.org/1742-6596/854/1/012040)

IOP Conf. Series: Journal of Physics: Conf. Series **854** (2017) 012040 doi:10.1088/1742-6596/854/1/012040

Large Eddy Simulation of an SD7003 Airfoil: Effects of Reynolds number and Subgrid-scale modeling

Hamid Sarlak

Fluid Mechanics Section, Department of Wind Energy, Technical University of Denmark, 2800 Kongens Lyngby, Denmark.

E-mail: hsar@dtu.dk

Abstract. This paper presents results of a series of numerical simulations in order to study aerodynamic characteristics of the low Reynolds number Selig-Donovan airfoil, SD7003. Large Eddy Simulation (LES) technique is used for all computations at chord-based Reynolds numbers 10,000, 24,000 and 60,000 and simulations have been performed to primarily investigate the role of sub-grid scale (SGS) modeling on the dynamics of flow generated over the airfoil, which has not been dealt with in great detail in the past. It is seen that simulations are increasingly getting influenced by SGS modeling with increasing the Reynolds number, and the effect is visible even at a relatively low chord-Reynolds number of 60,000. Among the tested models, the dynamic Smagorinsky gives the poorest predictions of the flow, with overprediction of lift and a larger separation on airfoils suction side. Among various models, the implicit LES offers closest pressure distribution predictions compared with literature.

1. Introduction

Over the past few years, studies have proved the capability of LES for airfoil simulations (cf. Mellen et al. [3]). Recently, a study was performed with the aim of investigating potential of LES in predicting the airfoil characteristics at high Reynolds numbers [1]. Uranga et al. [12] performed LES of the flow over a Selig-Donovan SD7003 airfoil for a range of Reynolds numbers between 10,000 and 60,000 at $\alpha = 4^o$, resulting in generation of laminar and fully turbulent flows over the airfoil, respectively. Recently, Sarlak et al. [8, 9] investigated aerodynamics of an S826 airfoil at low and moderate Reynolds numbers using LES and RANS methods.

While there has been a number of numerical studies for the flow past airfoils using LES techniques, an investigation of various subgrid scale models has not been studied extensively in the literature. The current paper investigates characteristics of the SD7003 airfoil at low Reynolds numbers and examines a number of SGS models in predicting the separation location, pressure distribution as well as airfoil polars.

2. Numerical Modeling

2.1. Governing equations

The flow is governed by Navier-Stokes equations which reads as

$$\frac{\partial \mathbf{v}}{\partial t} + \mathbf{v} \cdot \nabla \mathbf{v} = -\frac{\nabla p}{\rho} + \nabla \cdot [(\nu + \nu_{sgs}) \nabla \mathbf{v}], \quad (1)$$

where

$$\begin{aligned}
&\nu_{sgs} = 0 && \text{No model: implicit LES}\\
&\nu_{sgs} = c_s\Delta^2|\bar{S}| && \text{Mix-}S\text{: Mix-S}\\
&\nu_{sgs} = c_{ms}\Delta^{1.5}q_c^{0.25}|\bar{S}|^{0.5} && \text{Mix-}\omega\text{: Mix-O Dynamic}\\
&\nu_{sgs} = c_{mo}\Delta^{1.5}q_c^{0.25}|\bar{\Omega}|^{0.5} && \text{Smagorinsky: DynSmag,}
\end{aligned}$$

and ρ and ν are the fluid density and molecular viscosity, respectively. Also, $\mathbf{v}$ represents the filtered velocity vector, for simplicity called "valocity" from now on, and $p = p + (1/2)\rho u_j u_j$, is the modified pressure (it is pressure combined with the isotopic part of the subgrid-scale stress tensor which acts as a pressure). ν_{sgs} is the eddy viscosity to be specified by the SGS model. Four different SGS models are used to evaluate ν_{sgs}, as described in equation 1. Here, *NO model* refers to the case in which there is no explicit representation for turbulent viscosity and the only effects of kinetic energy dissipation are those arising from numerical dissipation. This case is included here as a measure of the relative impact of the SGS models. *Smagorinsky* refers to the standard Smagorinsky model, and *Mix-S* and *Mix-ω* represent the two variants of the mixed-scale model [5]. $q_c = (\bar{\tilde{u}_i} - \tilde{u}_i)^2$ is the sub-filter scale kinetic energy obtained by an explicit filtering (shown by bar) of larger size than the grid size, δ being the grid size, $\tilde{S}_{ij}(\mathbf{x}, t)$ and $\Omega = \nabla \times \tilde{u}(\mathbf{x}, t)$ are the resolved strain rate and vorticity, respectively. $c_s = 0.01$, $c_{mo} = 0.01$ and $c_{ms} = 0.06$ are (fixed) model constants used in the present study. The mixed-scale model is chosen in the existing code (see below) because of its low computational cost and its performance. Formally, it depends on the small scales through the term q_c (as a result of scale similarity) and on the resolved large scales through the resolved velocity gradient tensor. As a result, the model is able to predict a laminar flow close to the solid wall without a damping function.

2.2. Numerical solver

For the numerical simulations of the governing incompressible Navier-Stokes equations, the block structured general purpose flow solver, EllipSys3D [4, 11], is used in which the equations are discretized using a finite volume method for the primitive variables. Diffusive and convective terms are discretized using 2nd order central differencing schemes (CDS) and a blend of CDS and 3rd order QUICK scheme. Time is discretized using a second order backward Euler scheme and the solution is marched in time using inner time stepping. Pressure checker-boarding is prevented by using Rhie-Chow interpolation on a collocated grid arrangement and the pressure correction equation is solved using PISO algorithm.

3. Results

LES is used for all simulations and that four different subgrid scale (SGS) models are used for all simulations: a no-model (or implicit LES), dynamic Smagorinsky, as well as two variants of a mixed-scale SGS model referred to as Mix-O and Mix-S in [7] (for brevity, details of the models are not discussed in this paper). Following the meshing study [6] a numerical grid consisting of $1024 \times 256 \times 128$ cells in the streamwise direction, normal to the airfoil surface and along the span is used for the simulations. The span to chord ratio is set to 0.4. A non-dimensional time step of $t^* = dt.c/U_0 = 0.001$ is used in 40000 time steps and the statistics are time-averaged for the last 20000 time steps.

To validate current simulations, experimental results of [10] are used for the polars while the LES work of [2] is used to compare the pressure dstribution over airfoil. Figure 1 shows a comparison of lift polars where the simulations using the four various SGS models are being compared at angles of attack $\alpha = 4^o$ and $\alpha = 8^o$. As can be seen, at $\alpha = 4^o$ the agreement between LES and experiments is good for LES cases except the dynamic Smagorinsky which over-predicts the lift by a higher margin. At $\alpha = 8^o$, results of implicit LES and Mix-O model are nearly identical but dynamic Smagorinsky and Mix-S models overpredict and underpredict the

lift by around 10%, respectively. To further investigate the effect of SGS models, comparisons of flow structures using various models is presented in the following section.

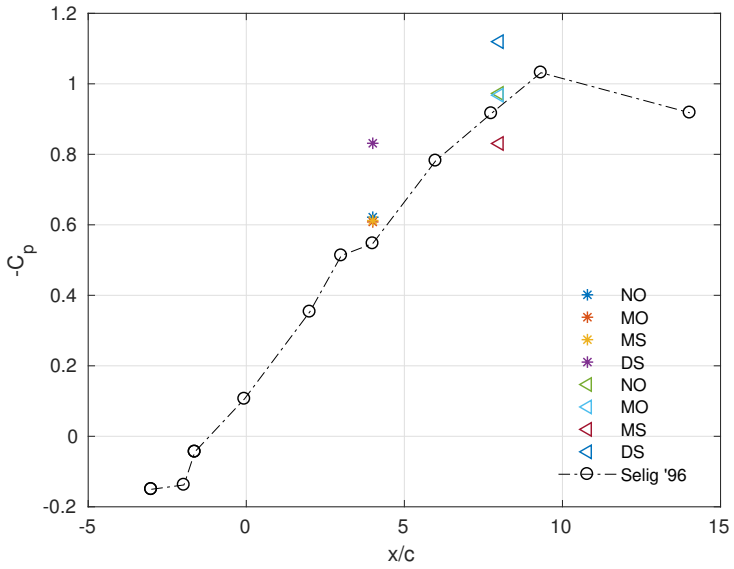

Figure 1. Lift polars for the SD7003 airfoil at Reynolds number 60,000. Comparison against experiments by Selig [10] are performed at $\alpha = 4^o$ and $\alpha = 8^o$.

3.1. Effect of angle of attack on velocity distribution over airfoil

To get an overview of the flow structures over the airfoil at various configurations, snapshots of flow past the airfoil at various angles of attack are plotted in figure 2. As can be seen, at $\alpha = 4^o$, the separation –shown by blue color, occurs at the middle of the chord and continues towards the trailing edge. By increasing angle of attack to $\alpha = 8^o$, laminar separation and flow re-attachment happens over the airfoil and at the two higher angles of attack, the flow undergoes leading edge separation which becomes stronger at $\alpha = 16^o$.

3.2. Effect of Reynolds number on the flow structures

Figure 3 presents the effect of Reynolds number on the flow attachment over the airfoil and subsequent aerodynamic loads. Two flow regimes at chord-based Reynolds numbers of Re=24,000 and Re=60,000 are investigated and flow past airfoil at angles of attack $\alpha = 4^o$, 8^o and 12^o are illustrated respectively. As can be seen, for all cases, the boundary layer gets thinner as a result of increasing the Reynolds number. At $\alpha = 4^o$ the Re=24,000 flow gets separated at nearly x/c=0.1 and exhibits recirculation further downstream whereas for the higher Reynolds number flow, a visible separation point is hardly seen. This is due to the dominance of higher momentum and its entrainment to the boundary layer to oppose adverse pressure gradients. At both $\alpha = 8^o$ and $\alpha = 10^o$, increasing the Reynolds number results in moving the separation point further upstream, with such phenomenon being more significant at $\alpha = 10^o$ where a separation bubble spanning the whole airfoil turns into one spanning about 15% of the chord.

3.3. Effect of SGS modeling on turbulence intensities and pressure and velocity distributions over airfoil

In order to quantify the effect of SGS modeling, one can first compare magnitude of the normalized viscosity, that is, eddy viscosity relative to the molecular viscosity. Figure 4 shows

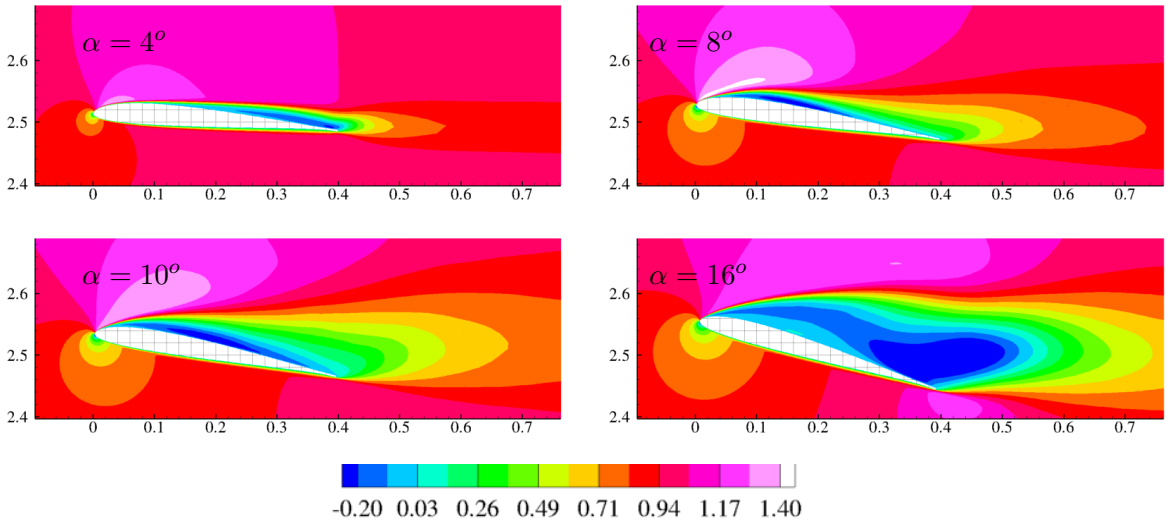

Figure 2. Mean streamwise velocity contours on the SD7003 airfoil for Reynolds number 24,000 at $\alpha = 4^o$, $\alpha = 8^o$, $\alpha = 10^o$, and $\alpha = 16^o$, respectively. x-axis: x/c, y-axis: y/c.

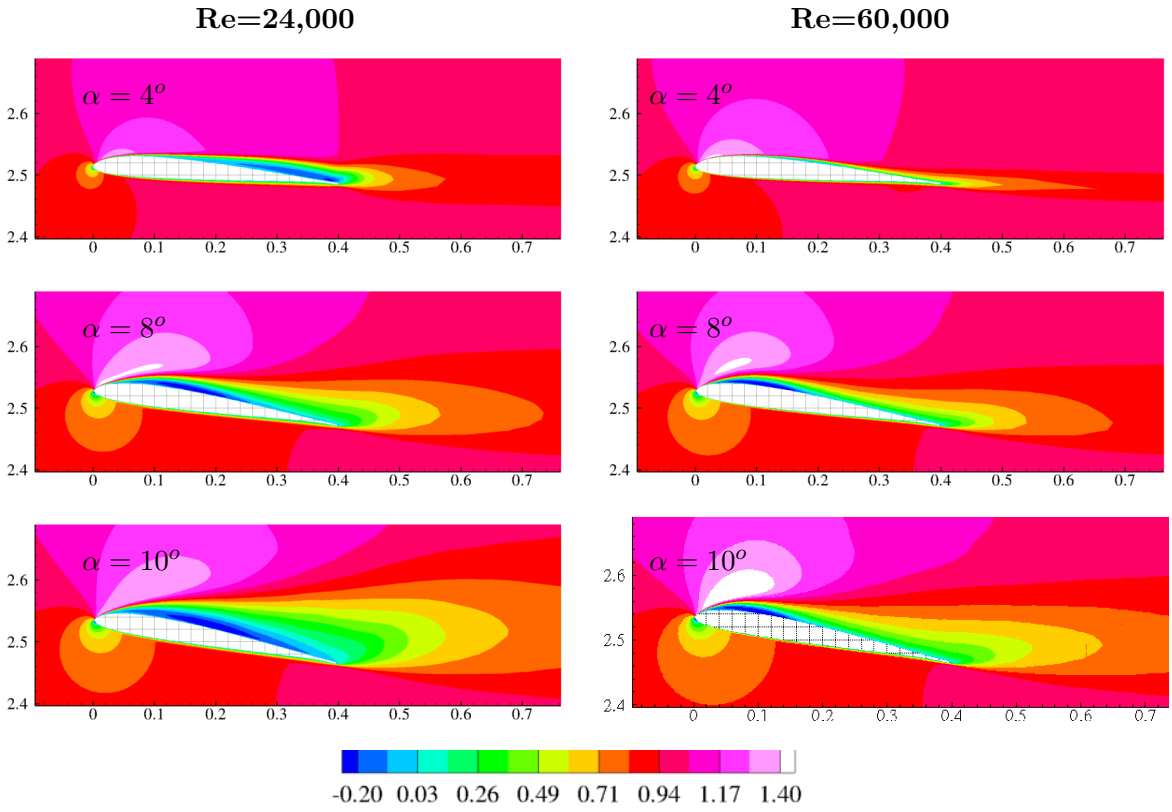

Figure 3. Mean streamwise velocity contours on the SD7003 airfoil for Reynolds numbers 24,000 (left) and 60,000 (right) at $\alpha = 4^o$ (top), $\alpha = 8^o$ (middle), and $\alpha = 10^o$ (bottom). Results are obtained using "MO" SGS model. x-axis: x/c, y-axis: y/c.

such quantities for the three Reynolds numbers (10,000, 24,000 and 60,000) at $\alpha = 4^o$. As can be seen, the normalized eddy viscosities are of the order of O(1), meaning that the contribution

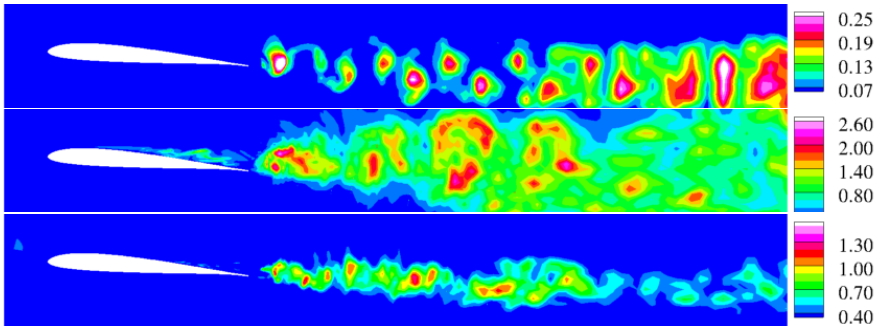

Figure 4. Effect of Reynolds number on turbulent viscosities. Normalized SGS viscosity contours on the SD7003 airfoil for Reynolds numbers 10,000 (top) and 60,000 (bottom) at $\alpha = 4^o$.

of the LES-generated viscosity is of the same order as the molecular viscosity. Looking at the color bar, note that the normalized values for Re=60,000 are approximately 6 times higher than Re=10,000. The trend at Re=24,000, however, suggests generally higher values of eddy viscosity than both lower and higher Reynolds numbers. While one explanation could be that at Re=24,000 flow starts exhibiting more violent fluctuations due to a transient nature, this trend needs to be investigated further.

To compare the different SGS models in predicting the flow past the airfoil, two sets of results at Reynolds numbers 10,000 and 60,000 are presented. Figure 5 illustrates the streamwise turbulence intensity $\sqrt{< u'u' >}/U_0$ contours obtained using the four SGS models for the case of Re=10,000 and figure 6 presents the same results for Re=60,000. Both cases demonstrate an angle of attack of $\alpha = 4^o$. As can be seen, even the effects of SGS model for the case of Re=10,000 are hardly noticeable. On the other hand, the SGS model for Re=60,000 can have a large impact on the quality of the results obtained. This is an interesting observation since the normalized eddy viscosity is of the order of unity for all of these cases and therefore one would imagine a much less impact of SGS models involved.

Comparison of various SGS models in streamwise velocity contours is also informative as it contains information about separation and recirculating flows on the suction side of the airfoil. Figures 7 and 8 illustrate the comparisons of velocity contours. Again, as can be imagined, at Re=10,000, results are insensitive to the SGS model whereas results of the Re=60,000 flow exhibit more significant differences. In particular, it is observed that among the four investigated models, the dynamic Smagorinsky presents a stronger separation point and recirculating flow towards the leading edge.

In order to better quantify the differences and compare against available references, pressure distribution over the airfoil at Re=60,000 is plotted in figure 9 for various SGS models at $\alpha = 4^o$. As can be noticed, there is a sizeable difference between model predictions. Interestingly, among various models, the implicit LES version predicts the flow separation and peak pressures almost dentical to the LES computations of Galbraith and Visbal [2]. The overprediction of lift using the dynamic Smagorinsky model that was observed in figure 1 can now be explained by the separation behaviour (particularly delayed reattachment) and the corresponding pressure distribution which results in higher area below the Cp curve. The wiggles on the curves are representing spanwise variation of pressure and are intentionally plotted to compare 3D effects visually. Clearly, all models except the Dynamic Smagorinsky predict quite a 2D pressure distribution over the airfoil on the suction side. It is also worthy to note how different is the behaviour of various models in capturing the laminar separation bubble - size and location.

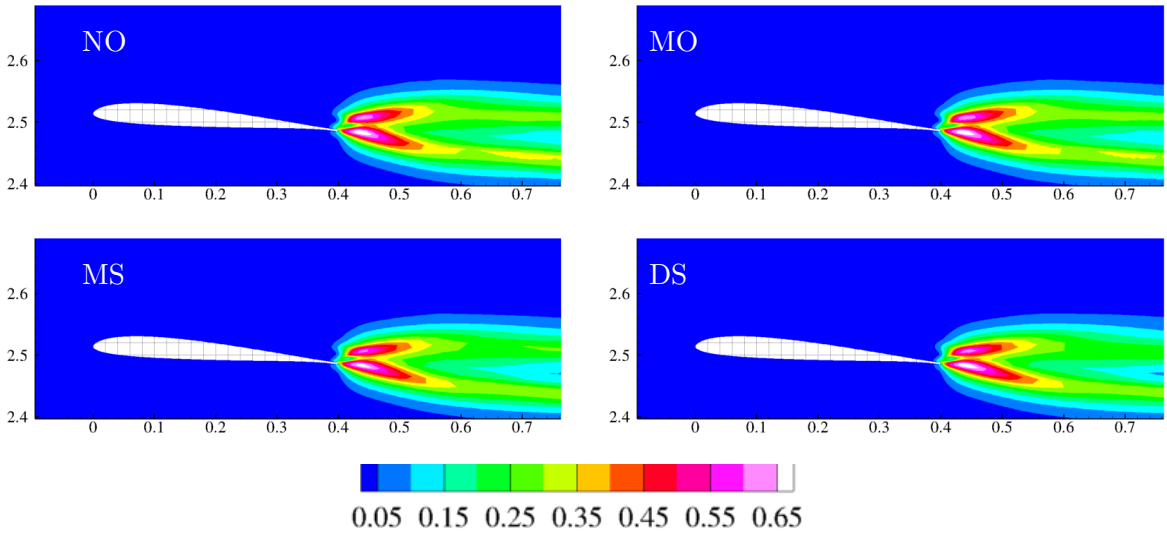

Figure 5. Effect of SGS modeling on the predicted streamwise turbulence intensity contours on the SD7003 airfoil for Reynolds number 10,000 obtained using various SGS models at $\alpha = 4^o$. NO: implicit (no model) LES, MO: Mix-Ω, MS: Mix-S, DS: dynamic Smagorinsky, as in [7]. x-axis: x/c, y-axis: y/c.

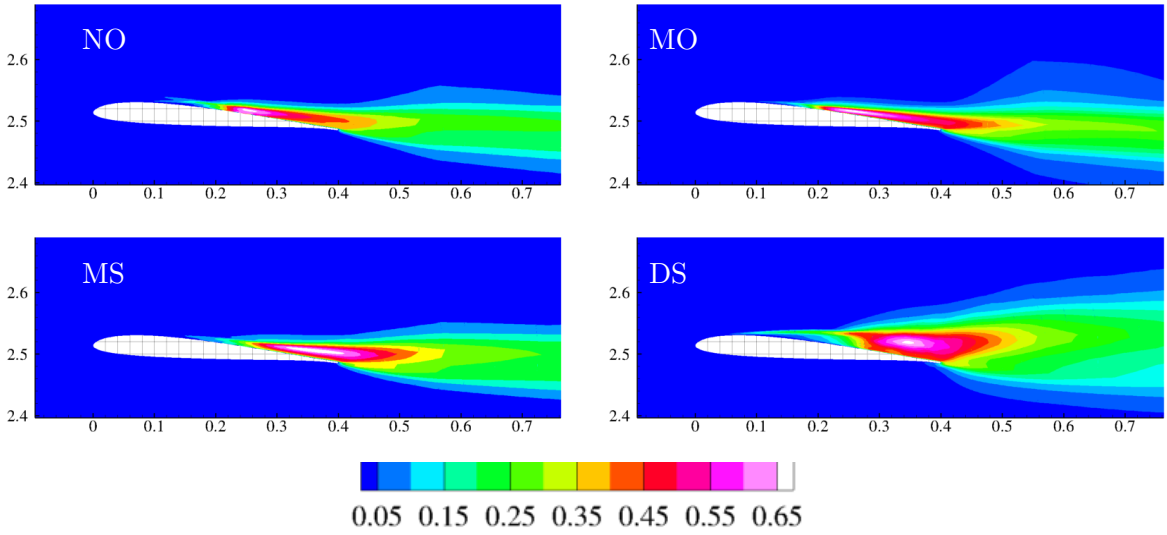

Figure 6. Effect of SGS modeling on the predicted streamwise turbulence intensity contours on the SD7003 airfoil for Reynolds number 60,000 and angle of attack $\alpha = 4^o$ using various SGS models. NO: implicit (no model) LES, MO: Mix-Ω, MS: Mix-S, DS: dynamic Smagorinsky, as in [7]. x-axis: x/c, y-axis: y/c.

4. Conclusions

Large Eddy Simulation of an SD7003 airfoil at low Reynolds numbers was performed at various angles of attack at chord-Reynolds numbers of Re=10,000, Re=24,000 and Re=60,000 in order to assess the applicability of four SGS models and investigate their role in predicting turbulence at different flow regimes.

The effect of Reynolds number on the flow behavior was investigated and it was seen that

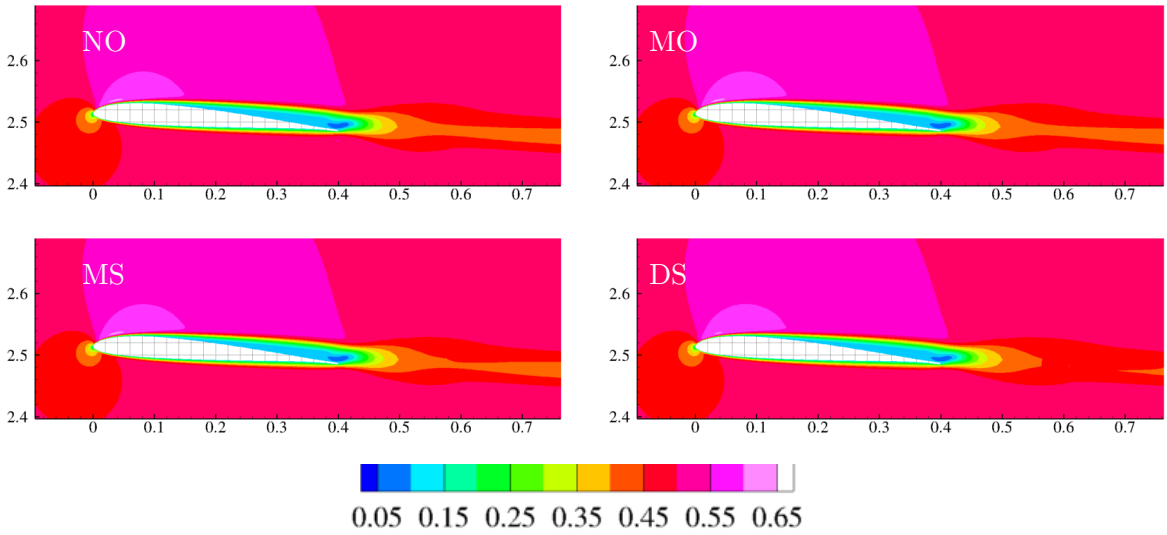

Figure 7. Effect of SGS modeling on the predicted mean streamwise velocity contours on the SD7003 airfoil for Reynolds number 10,000 obtained using various SGS models. NO: implicit (no model) LES, MO: Mix-Ω, MS: Mix-S, DS: dynamic Smagorinsky, as in [7]. x-axis: x/c, y-axis: y/c.

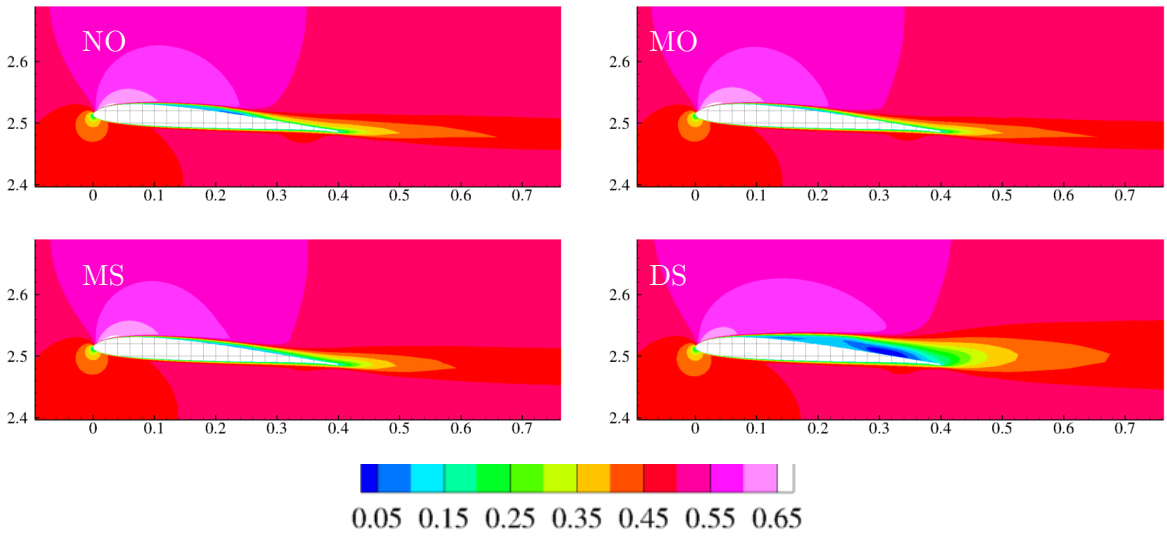

Figure 8. Effect of SGS modeling on the predicted mean streamwise velocity contours on the SD7003 airfoil for Reynolds number 60,000 obtained using various SGS models. NO: implicit (no model) LES, MO: Mix-Ω, MS: Mix-S, DS: dynamic Smagorinsky, as in [7]. x-axis: x/c, y-axis: y/c.

increasing Reynolds number results in shrinking the separation bubble that is formed on airfoil's suction side and moving the separation point towards the leading edge.

Through the study of four different SGS models at different Reynolds numbers, it was seen that at Re=10,000 the SGS models predict almost identical flow structures, whereas with increasing the Reynolds number to 60,000, the results vary among the different models. This is in contraty to the less-sensitive results of actuator line simulations presented in [7], mainly due to

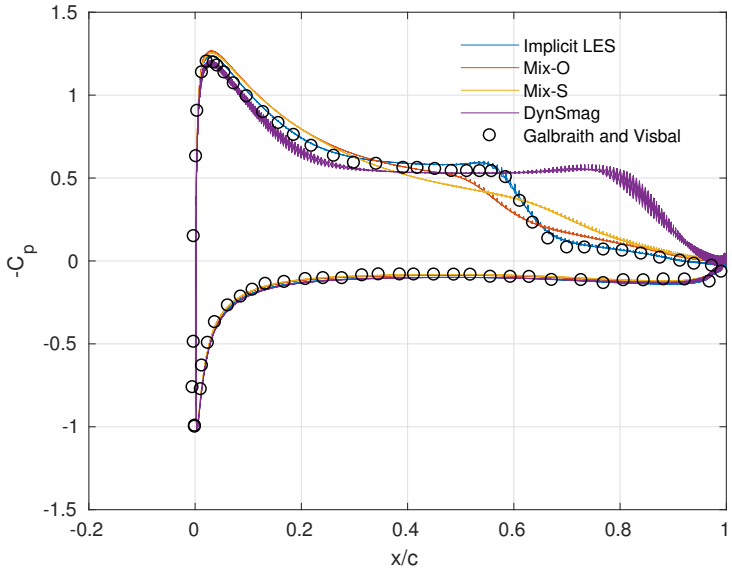

Figure 9. Pressure coefficient distribution over the SD7003 airfoil at Reynolds number 60,000 using $\alpha = 4^o$ and comparison against Galbraith and Visbal [2].

the presence of solid surfaces. In particular, the dynamic Smagorinsky model seemed to predict an earlier and stronger separation followed by a stronger wake and higher turbulence levels which eventually led to overprediction of lift. A more detailed comparison of the instantaneous results for spectral analysis of the signals would shed more light on the origin of the discrepancies. This will be performed in a future study.

References

[1] L. Davidson. *LESFOIL: Large Eddy Simulation of Flow Around a High Lift Airfoil: Results of the Project LESFOIL Supported by the European Union 1998-2001*, volume 83. Springer, 2003.

[2] Marshall Galbraith and Miguel Visbal. Implicit large eddy simulation of low-reynolds-number transitional flow past the sd7003 airfoil. In *40th Fluid Dynamics Conference and Exhibit*, page 4737.

[3] CP. Mellen, Fröhlich J., and W. Rodi. Lessons from lesfoil project on large-eddy simulation of flow around an airfoil. *AIAA journal*, 41(4):573–581, 2003.

[4] JA. Michelsen. *Basis3D-a platform for development of multiblock PDE solvers.* PhD thesis, Technical Note AFM92-05, Technical University of Denmark, Department of Fluid Mechanics, 1992.

[5] P. Sagaut. *Simulations numériques d'écoulements décollés avec des modèles de sous-maille.* PhD thesis, 1995.

[6] H. Sarlak. *Large eddy simulation of turbulent flows in wind energy.* PhD thesis, Technical University of Denmark, 2014.

[7] H Sarlak, C Meneveau, and JN Sørense. Role of subgrid-scale modelling in large eddy simulation of wind turbine wake interactions. *Renewable Energy*, 77:386–399, 2015.

[8] H. Sarlak, R. Mikkelsen, S. Sarmast, and JN. Sørensen. Aerodynamic behaviour of nrel s826 at re=100,000. *Journal of Physics, Conf. Series*, 524(1):012027, 2014.

[9] H Sarlak, T Nishino, Jens Nørkær Sørensen, Theodore Simos, and Charalambos Tsitouras. Urans simulations of separated flow with stall cells over an nrel s826 airfoil. In *AIP Conference Proceedings*, volume 1738, page 030039. AIP Publishing, 2016.

[10] MS. Selig, CA. Lyon, P. Giguere, C. Ninham, and JJ. Guglielmo. *Summary of low-speed airfoil data*, volume 2. SoarTech Publications, 1995.

[11] NN. Sørensen. *General purpose flow solver applied to flow over hills.* PhD thesis, Technical University of Denmark, Risø National Laboratory for Sustainable Energy, 1995.

[12] A. Uranga, PO. Persson, M. Drela, and J. Peraire. Implicit large eddy simulation of transitional flows over airfoils and wings. *Proceedings of the 19th AIAA Computational Fluid Dynamics, no. AIAA*, 4131, 2009.